

Natural Cold Baryogenesis from Strongly Interacting Electroweak Symmetry Breaking

Thomas Konstandin^a and G eraline Servant^{a,b}

^a*CERN Physics Department, Theory Division, CH-1211 Geneva 23, Switzerland*

^b*Institut de Physique Th eorique, CEA/Saclay, F-91191 Gif-sur-Yvette C edex, France*

tkonstan@cern.ch, geraldine.servant@cern.ch

Abstract

The mechanism of “cold electroweak baryogenesis” has been so far unpopular because its proposal has relied on the ad-hoc assumption of a period of hybrid inflation at the electroweak scale with the Higgs acting as the waterfall field. We argue here that cold baryogenesis can be naturally realized without the need to introduce any slow-roll potential. Our point is that composite Higgs models where electroweak symmetry breaking arises via a strongly first-order phase transition provide a well-motivated framework for cold baryogenesis. In this case, reheating proceeds by bubble collisions and we argue that this can induce changes in Chern-Simons number, which in the presence of new sources of CP violation commonly lead to baryogenesis. We illustrate this mechanism using as a source of CP violation an effective dimension-six operator which is free from EDM constraints, another advantage of cold baryogenesis compared to the standard theory of electroweak baryogenesis. Our results are general as they do not rely on any particular UV completion but only on a stage of supercooling ended by a first-order phase transition in the evolution of the universe, which can be natural if there is nearly conformal dynamics at the TeV scale. Besides, baryon-number violation originates from the Standard Model only.

Contents

1	Introduction	1
2	Cold electroweak baryogenesis	3
3	Preheating after a relativistic first-order phase transition	6
4	Estimate of the baryon asymmetry	12
5	Conclusion	14

1 Introduction

There are two major approaches to explain the matter-antimatter asymmetry of the universe. One is called *leptogenesis*, in which case the asymmetry is produced by the decay of right-handed neutrinos in the early universe. The underlying assumptions are that neutrinos are Majorana particles and that the reheating temperature of the universe has to be at least $\sim 10^{11}$ GeV. Leptogenesis is theoretically well-motivated (for a review see e.g. [1]), the main drawback is the difficulty to test this mechanism, in particular because the CP violation involved in this process does not manifest itself in low-energy experiments. The fact that the required reheating temperature of the universe is quite large may also be a concern, as we will further develop in this paper.

A second avenue, the so-called *electroweak baryogenesis* mechanism [2], is to consider that the matter-antimatter asymmetry has nothing to do with lepton number violation and is produced at the electroweak (EW) epoch [3]. In this case, the sole source of baryon number violation is from the Standard Model sphalerons. Since sphaleron processes are at thermal equilibrium before the electroweak phase transition and are exponentially suppressed in the EW broken phase as $\sim \exp\left(-\sqrt{\frac{4\pi}{\alpha_w}}\mathcal{C}\frac{\langle\phi(T)\rangle}{T}\right)$, where $1.5 \lesssim \mathcal{C} \lesssim 2.7$ depends on the Higgs mass, the common lore is that an asymmetry can only be generated during the EW phase transition, provided that it is first-order. The process is non-local as it relies on charge transport in the vicinity of the CP-violating bubble walls. Because it involves EW scale physics only, this mechanism is particularly appealing and will start to be tested at the LHC. While it is relatively easy to modify the Higgs potential so that the EW phase transition is strongly first-order, a main difficulty of EW baryogenesis is that it requires large new sources of CP violation which are typically at odds with experimental constraints from electric dipole moments.

EW baryogenesis has been investigated in detail mostly in the Standard Model [4] (where it is excluded by now [5, 6]) and its supersymmetric extension [7–11]. The nature of the EW phase transition has also been studied in models of technicolor [12], although no full calculation of the asymmetry has been carried out in this context. The starting observation for this paper is that in models where the EW symmetry is broken by strong dynamics, the EW phase transition is typically too strongly first-order [13–16], leading to supersonic bubble growth which suppresses diffusion of CP violating densities in front of the bubble walls, thus preventing the mechanism of EW baryogenesis [17]. Our goal is to revive another mechanism,

known as *cold baryogenesis* [18–28] and show that it is theoretically well-motivated and only relies on the existence of a nearly conformal sector at the TeV scale, something which will be tested at the LHC. Our conclusions will be general and model-independent. One major advantage of cold baryogenesis is that it does not depend on the details of the new sources of CP violation, which can be described by dimension-six effective operators which are totally unconstrained by EDMs.

The cold baryogenesis mechanism is interesting in that it also only invokes Standard Model baryon number violation and beautifully makes use of the global texture of the $SU(2)$ electroweak theory. Nevertheless, so far, it has not received too much acclaim because it relies on a somewhat unnatural assumption: a period of low-scale (EW scale) hybrid inflation with the Higgs as the waterfall field. The end of inflation is triggered when the Higgs mass turns negative and a spinodal instability gives rise to an exponential growth of soft Higgs modes. At this stage, all particles present before low scale inflation have been inflated away and the universe is cold and empty. Subsequently, the vacuum energy stored in the Higgs and inflaton fields reheats the plasma. This energy transfer happens far away from equilibrium, which makes baryogenesis during this period feasible. One of the weaknesses of this scenario is that low scale inflation requires a significant amount of tuning in the inflaton sector [20, 25, 28]. Besides, like for the Higgs, a fundamental light scalar inflaton implies a hierarchy problem.

The purpose of the present paper is to demonstrate that the conformal phase transition in some models of strongly coupled electroweak symmetry breaking can lead quite generically to a situation in which cold electroweak baryogenesis is feasible. We want to keep the discussion as model-independent as possible. In addition to a nearly conformal potential for the dilaton, we only need to assume a sizable coupling between the dilaton and the Higgs as well as a slightly larger potential energy associated with the dilaton. Let us for instance consider a scalar potential of the type

$$V(\mu, \phi) = \mu^4 \times \left(P((\mu/\mu_0)^\epsilon) + \mathcal{V}(\phi)/\mu_0^4 \right), \quad (1)$$

where μ is the canonical radion (dilaton) field which acquires a vev $\mu_0 \sim \mathcal{O}(1 \text{ TeV})$. At the confining scale μ_0 , an approximate conformal symmetry governs the dynamics. $|\epsilon|$ parametrizes the explicit breaking of conformal invariance and we are working in the limit $|\epsilon| \ll 1$ leading to a very shallow potential $P((\mu/\mu_0)^\epsilon)$ with widely separate extrema. The Randall–Sundrum model [29] with Goldberger–Wise stabilization [30] is an explicit realization of this scenario where the stabilization of a warped extra dimension solves the hierarchy problem. It is dual, via the AdS/CFT correspondence, to a 4D theory where confinement is induced by an interplay of weakly coupled operators perturbing a CFT [31, 32]. As well-known from lattice studies, confining phase transitions are first-order for the rank of the $SU(N)$ gauge group $N \gtrsim 3$ (the exact bound depends on the matter content) and growing more strongly first-order as N increases.

For our discussion, we do not need to specify the form of the Higgs potential $\mathcal{V}(\phi)$, which can be Standard-Model like. The cosmological properties of the potential (1) are reviewed in a companion article [33]. The radion acts in this context similar to an inflaton and the conformal symmetry protects the Higgs as well as the radion mass thus solving the hierarchy problem. For example, let us consider the Randall-Sundrum scenario with the 5D warped metric $ds^2 = e^{-2r/l} \eta_{\rho\sigma} dx^\rho dx^\sigma + dr^2$ (the radion field is then defined as $\mu = l^{-1} e^{-r/l}$ where

$l \sim M_{Pl}^{-1}$ is the AdS_5 curvature) and with the Standard Model Higgs field φ on the infrared brane. Because the radion arises as a gravitational degree of freedom, its coupling to the Higgs arises from the induced metric on the IR brane. The resulting 4D effective action for the Higgs is then:

$$\mathcal{L}_4 = \frac{\mu^2}{\mu_0^2} g^{\rho\sigma} D_\rho \phi D_\sigma \phi - \frac{\mu^4 \lambda}{\mu_0^4 4} (\phi^2 - v_0^2)^2 \quad (2)$$

where the Higgs φ has been redefined as $\phi = \mu_0 l \varphi$ and $v_0 = \mu_0 l v$ where $v \sim M_{Pl}$. We recover the second term in the potential (1) although for a non-canonical Higgs field ϕ . In the limit $\langle \mu \rangle \rightarrow 0$, one can easily see that the vev of the canonical Higgs is proportional to μ and therefore $\langle \mu \rangle$ sets the EW scale. We also note that in the case of a little hierarchy $\mu_0 > v_0$, we can neglect the Higgs contribution when studying the dynamics of the radion. In general (for instance if the Higgs is delocalized towards the bulk), the interactions between the Higgs and the radion will be different from (2) but this should not affect much our discussion. What we rely on in this paper is that the conformal phase transition leading to $\langle \mu \rangle \neq 0$ is strongly first-order and proceeds by bubble nucleation. This modifies significantly the standard picture of reheating.

In the next section, we review the microscopic picture of cold electroweak baryogenesis. In Section 3 we discuss preheating after a stage of supercooling ended by a strongly first-order phase transition and argue that models with nearly conformal dynamics offer all the required conditions for successful cold baryogenesis. We estimate the resulting baryon asymmetry in Section 4 and conclude in Section 5.

2 Cold electroweak baryogenesis

The main idea of cold baryogenesis relies on the evolution of winding number and Chern-Simons number in a fast tachyonic EW transition. In the ‘standard’ picture (see e.g. [19]), the EW phase transition is triggered by a rapid change in the Higgs mass (“quenching”) in a nearly empty Universe. This can be arranged for instance in a low-scale inverted hybrid inflation scenario where the inflaton is coupled to the Higgs [34, 35, 22–24]. The resulting tachyonic instability leads to strongly out-of-equilibrium conditions with an exponential growth of occupation numbers in the Higgs fields and after a short while the system becomes classical. The $SU(2)$ orientation of the Higgs field is inhomogeneous in space such that different regions approach different minima in the Higgs potential, similar to a spinodal decomposition. The dynamics of the system can lead to substantial changes in the Chern-Simons number of the $SU(2)$ gauge fields

$$N_{CS} = -\frac{1}{16\pi^2} \int d^3x \epsilon^{ijk} \text{Tr} \left[A_i \left(F_{jk} + \frac{2i}{3} A_j A_k \right) \right], \quad (3)$$

and can therefore induce baryon number violation via the quantum anomaly that relates a change in baryon number B to a change in Chern-Simons number N_{CS}

$$\Delta B = 3\Delta N_{CS}. \quad (4)$$

The key point is that the dynamics of the Chern-Simons number is linked to the dynamics of the Higgs field via the Higgs winding number

$$N_H = \frac{1}{24\pi^2} \int d^3x \epsilon^{ijk} \text{Tr} [\partial_i \Omega \Omega^{-1} \partial_j \Omega \Omega^{-1} \partial_k \Omega \Omega^{-1}], \quad (5)$$

where Ω is given by the elements of the usual $SU(2)$ Higgs doublet ϕ of the SM :

$$\frac{\rho}{\sqrt{2}} \Omega = (\epsilon \phi^*, \phi) = \begin{pmatrix} \phi_2^* & \phi_1 \\ -\phi_1^* & \phi_2 \end{pmatrix}, \quad \rho^2 = 2(\phi_1^* \phi_1 + \phi_2^* \phi_2). \quad (6)$$

Both the winding number and the Chern-Simons number change under large gauge transformations. However, the variations ΔN_{CS} , ΔN_H and the difference

$$\delta N \equiv N_{CS} - N_H, \quad (7)$$

are gauge invariant. In the vacuum, $\delta N = 0$. A texture is a configuration which has $\delta N \neq 0$, with a Higgs length ρ that is equal to its vacuum value everywhere and which only carries gradient energy. In the absence of gauge fields, textures are not stable configurations but shrink quickly [36] and the vacuum configuration is the constant Higgs field with vanishing winding number.

Cold EW baryogenesis is based on gauged textures of the EW gauge sector of the SM [37]. A gauged texture is also unstable and its evolution depends on its length scale L . A localized texture just collapses by changing N_H , in which case baryon number is not violated. However, if textures are spread out and larger than the size of gauge fields $\sim m_W^{-1}$, gauge fields can cancel the Higgs gradient energy and textures decay by changing the Chern-Simons number (thus producing baryon number) [38]. For example, consider the configuration

$$\Omega(x_\mu) = \frac{\mathbf{1}L + \sigma_i(x_i - x_i^0)}{\sqrt{L^2 + (x - x^0)^2}}, \quad (8)$$

which carries a non-trivial winding number (σ_i are the Pauli matrices, L parametrizes the size of the configuration and x_i its position). In order to produce such a configuration out of a trivial one ($\Omega = \mathbf{1}$), the Higgs field has to surpass a potential barrier. While the winding number of the configuration (8) is rather homogeneously spread in space, roughly half of the winding is localized near the position of the Higgs zero for a configuration that is close to surpassing the barrier [26]. This ‘half-knot’ changes sign when the barrier is surpassed in a way that changes the total Higgs winding by one unit. Since the system has to approach the vacuum at later stages, the Higgs winding has to either decay ($L \rightarrow \infty$) or be dressed by the gauge fields ($A_i \rightarrow \partial_i \Omega \Omega^{-1}$). In the latter case, this leads to a change in Chern Simons number, hence a change in baryon number.

The inflaton dynamics can lead to a parametric resonance (preheating) when large amplitude non-thermal excitations in both the inflaton and coupled Higgs field arise. During the EW phase transition and the following preheating stage, $\delta N \neq 0$ configurations are then abundantly produced. They eventually relax to zero. However, in the presence of CP violation, $\delta N > 0$ and $\delta N < 0$ winding configurations which have a size comparable to m_W^{-1} evolve differently towards the vacuum. $\delta N < 0$ windings have a slight preference to relax by

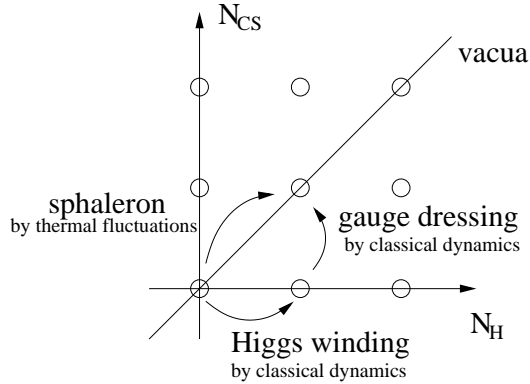


Figure 1: In standard EW baryogenesis, baryon number violation occurs via high temperature induced sphaleron transitions, along the “vacua” line $N_H = N_{CS}$. In contrast, in cold baryogenesis, sphaleron transitions are switched off and baryon number violation takes place in a two-step process via the production and decay of textures (configurations having $N_H \neq N_{CS}$). First, large kinetic energy stored in the scalar sector induces Higgs winding transitions. Second, these winding configurations can decay by changing Chern-Simons number, thus producing baryon number.

changing N_H while $\delta N > 0$ configurations have a slight preference to unwind by changing N_{CS} . The imbalance between a change in winding number and a change in Chern-Simons can then generate a net baryon number under out of equilibrium conditions.

A common source of CP violation employed in this context is the higher dimensional operator¹

$$\mathcal{O}_{CPV} = \frac{1}{M^2} \phi^\dagger \phi \tilde{F} F, \quad (9)$$

which acts as a chemical potential for Chern-Simons number and yields the required bias towards baryon number generation. A major advantage of an operator of the form (9) is that the observed baryon asymmetry can be explained without conflicting with constraints from electric dipole moments.

Because of the non-perturbative nature of the phenomenon, it is difficult to derive reliable analytical estimates for the baryon asymmetry. However, a nice feature of cold EW baryogenesis is that most of the process can be simulated on a computer lattice (from the very early to the very late stages) [39, 34, 35, 22–24]. In particular, the behavior of winding and Chern-Simons number can be explicitly observed [26].

A crucial ingredient for a successful baryogenesis mechanism is to prevent washout of the baryon asymmetry which is possible if the tachyonic transition takes place in a cold universe. This is generally achieved by engineering a low scale inflaton coupled to the Higgs. Our goal in this paper is to show that there is another natural and well-motivated route for implementing cold baryogenesis: a nearly conformal phase transition at the TeV scale.

To conclude this section, we point out that an earlier proposal for *local* EW baryogenesis (in which B and CP occur together in space and time) based on the decay of textures

¹Operators obtained by integrating out the SM fermions [40–43] have also been advocated as efficient CP violating sources for cold EW baryogenesis [44, 45]. However, the validity of the approach can be questioned due to the role of hard modes in the generation of winding number (i.e. harder than the charm or strange quark mass which is the inverse of the expansion parameter in [43]). Furthermore, the operators of [43] could not be reproduced using different techniques [46, 47].

was made in Ref. [37, 48, 49, 38]. It assumed a first-order EW phase transition, proceeding through the nucleation and expansion of bubbles filled with the new (broken) phase. The idea was based on the production and decay of configurations carrying non-vanishing winding number while the passing bubble wall drives the system out-of-equilibrium. It was however later shown that this mechanism does not lead to a sufficient baryon asymmetry [38]. This problem was cured in the so-called *non-local* (by charge transport) and now standard EW baryogenesis mechanism [50] where CP violation originates in the fermionic sector and is transported by diffusion into the symmetric phase where sphaleron transitions are unsuppressed and biased by the CP-violating fermion densities, thus producing the baryon asymmetry. However, in this case, the asymmetry is produced at high temperature and leads to strong constraints on the finite temperature Higgs potential nature via the sphaleron bound $\phi/T \gtrsim 1$ where ϕ and T are evaluated at the nucleation temperature. In contrast, in cold baryogenesis, the EW phase transition takes place at very low temperature (and does not have to be first-order). ΔB generation in cold and standard cases are sketched in Fig. 1.

3 Preheating after a relativistic first-order phase transition

For cold electroweak baryogenesis to be viable, one has to ensure that in the first stage of the reheating process, most of the energy resides in the scalar sector with momenta of the order of the electroweak scale before the system approaches equilibrium. This is the topic of this section. We have seen earlier that at the EW symmetry breaking transition, the Higgs field produces winding as it falls towards the vacuum. Ignoring gauge fields, winding configurations collapse and unwind. In a gauge theory, the behavior of textures is more complex. The tendency of the Higgs field to unwind is competed by the gauge fields which can cancel gradient energy in the Higgs field. In particular, if the initial size L of the winding configuration is $L < m_W^{-1}$ the gradient term in the Higgs field is large and pulls the Higgs field over the potential barrier and changes N_H to match N_{CS} whereas if $L > m_W^{-1}$ the gauge field changes winding number to match N_H . To produce baryon number, we need to change the value of N_{CS} so what is crucial is to determine under which conditions winding configurations can be produced during a first-order phase transition and what is their typical size. The first-order phase transition we have in mind refers to the conformal phase transition described in detail in [33] which implies that the induced electroweak symmetry breaking can take place at a temperature below the sphaleron freeze-out temperature. Since the radion vev induces a Higgs vev, the bubbles should be understood as both radion and Higgs bubbles.

Before percolation, the energy budget of a first-order phase transition depends on several factors such as the amount of latent heat released or the friction in the bubble wall [17]. Part of the energy is transformed into bulk motion and heat in front of the wall or is absorbed by the particles that climb the potential well induced by the changing scalar field vev. These are the microscopic processes that counteract the expansion of the bubble walls and constitute the friction felt by the scalar field. However, in the case of interest, the universe is cold and almost empty when the phase transition occurs such that the surrounding plasma cannot efficiently hinder the wall expansion and most of the energy is used to accelerate the wall [51], quite similarly to the situation in vacuum [52]. After some time of expansion, the walls are

highly-relativistic and since their size at the end of the phase transition is of order of the Hubble constant they can reach velocities of order $\gamma_w \sim (m_{Pl}/m_W)^{1/2} \sim 10^8$.

At the end of the phase transition, most of the energy of the system is localized in the expanding bubbles. Ultimately, when the bubbles start to collide and percolate this energy has to reheat the universe in a feasible cosmological scenario in order to reproduce the predictions of big bang nucleosynthesis. There are competing effects that are relevant in this era of equilibration, as e.g. particle production [53] or production of classical scalar waves [54, 53, 55, 56] by reflection of the coherent bubble walls.

Let us consider the production rate of a fermionic species that interacts with the scalar field ϕ via a Yukawa interaction during bubble collisions

$$\mathcal{L} \ni g \bar{\psi} \phi \psi. \quad (10)$$

The number of particles produced per area is [53]

$$\frac{N}{A} = 2 \int \frac{dk d\omega}{(2\pi)^2} |\phi(\omega, k)|^2 \text{Im}\Gamma^{(2)}(\omega^2 - k^2), \quad (11)$$

where $\phi(\omega, k)$ denotes the Fourier transform of the Higgs field configuration and $\Gamma^{(2)}$ denotes the second derivative of the effective action that in perturbation theory to leading order is given by

$$\text{Im}\Gamma^{(2)}(p^2) = \frac{g^2 p^2}{8\pi} \left(1 - \frac{4m^2}{p^2}\right)^{3/2} \Theta(p^2 - 4m^2), \quad (12)$$

for a fermion ψ of mass m . We use in the following this expression to estimate the energy that is transferred into the fermionic sector during reheating.

The production of sufficient Higgs winding number requires sizable kinetic energy in the Higgs field in the form of classical configurations that can surpass the potential barrier. This is prohibited if the energy of the scalar sector is drained too fast into fermions. How efficient scalar wave and fermion production is depends crucially on the vacuum structure of the scalar sector and in the following we will discuss three relevant cases in the limit of highly relativistic bubble wall velocities, $\gamma_w \rightarrow \infty$, namely

- (a) a periodic potential
- (b) a potential with two nearly degenerate minima
- (c) a potential with two asymmetric minima

During the phase transition the dynamics of both fields, Higgs and radion, are in principle important. The Higgs is most important for the generation of the baryon asymmetry via Higgs winding and Chern-Simons number. On the other hand, the radion will dominate the dynamics of the phase transition due to a slightly larger energy scale. Hence, whether the system goes back to the symmetric phase after the collision depends mostly on the features of the radion potential. In the following, we identify the scalar potential under consideration with the nearly conformal radion potential that belongs to the last category above.

First, if the vacuum structure is periodic, colliding bubble walls do not reflect and pass freely each other without interfering much (see Fig. 2(a)). Energy is very slowly carried

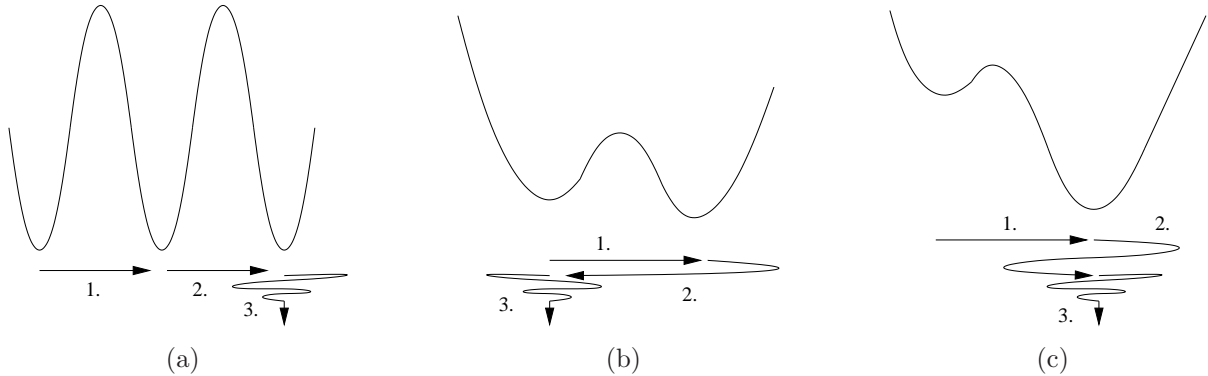


Figure 2: The path of the scalar field for the three different potentials a), b), c) discussed in the text. “1” denotes the path in the expanding bubble walls. “2” is the path during the collision. “3” is the path in the collided region.

over from walls to the scalar (radion and Higgs) sector. Most of the energy decays into SM particles before it is accumulated in the scalar sector. Besides, particle production is suppressed by the Lorenz factor γ_w^2 of the colliding bubble walls [53].

Secondly, in the case (b) where the scalar potential has two nearly degenerate local minima, the expanding bubble walls bounce in the potential and reflect at each other (see Fig. 2(b)). This reestablishes a region of symmetric phase between the collided bubble walls. The expansion of the bubble walls is counteracted by the pressure difference, such that the bubble walls are slowed down and finally the symmetric phase collapses again (as shown in Ref. [53] and in the left plots of Fig. 3 and Fig. 4). Each collision releases some fraction of the wall energy into scalar waves. Most of the energy is radiated away after a few collisions. Even though expanding bubble walls do not decay into fermions², thermalization occurs by production of scalar waves. The different collisions are separated by a time of the order of the Hubble time, which is much longer than the electroweak time scale that determines the decay rate of the classical scalar waves³. This constitutes a serious problem for us since the process of transferring the bubble wall energy into EW scale scalar configurations is very inefficient. On top of that, the reflections of bubble walls themselves lead to significant particle production: a fixed fraction g^2 of the energy of the colliding walls goes into production of fermions [53], even in the limit $\gamma_w \rightarrow \infty$. Hence, in the case of nearly degenerate vacua, a sizable fraction of the energy will be drained into the fermionic sector. Therefore, it is questionable that a sizable energy fraction is present in the form of classical kinetic energy of the Higgs field.

The potential (c) with two asymmetric minima gives different results. When two scalar bubbles collide, the scalar field bounces and is reflected close to the symmetric phase. However, a partial loss in energy implies that the field only approaches the old minimum to a certain extent. In Ref. [57, 58], it is shown that the walls are reflected only if the field can reach the basin of attraction of the symmetric minimum. If not, the field bounces back close to the symmetric minimum but remains in the basin of attraction of the broken phase. In

²This can be seen by noting that the wall profile has no time-dependence in the co-moving frame and only a support for $p^2 \leq 0$ in Fourier space. Hence there is no particle production according to (11).

³Using (11) the decay rate of the classical Higgs waves is basically the one of the Higgs particle.

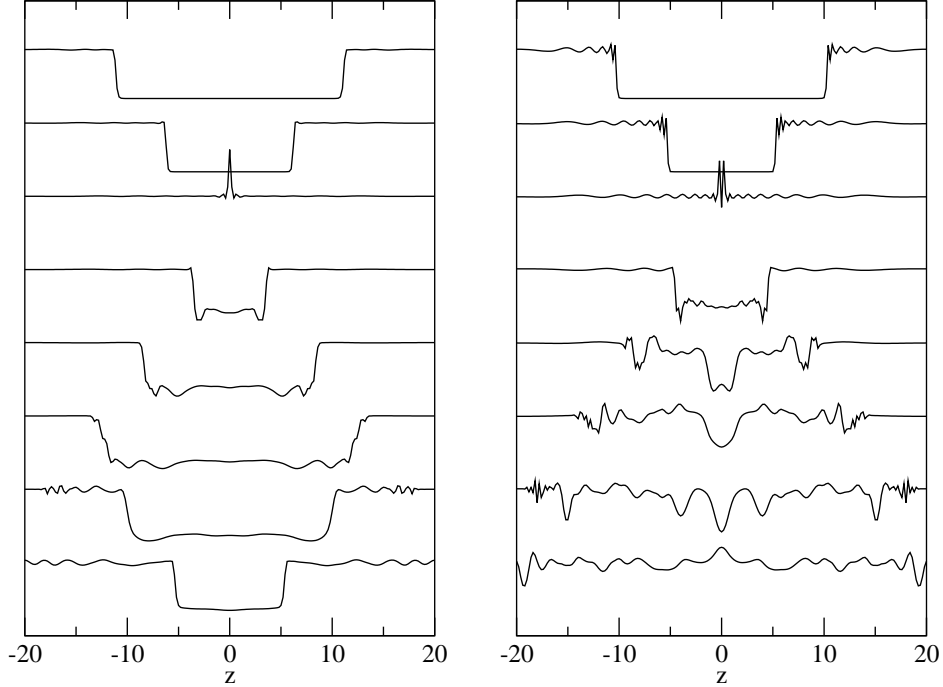


Figure 3: Collision of planar bubble walls (with initial velocity $v_w = 0.5$) using the potential (13) for $\lambda = 1$. The left (right) plots are respectively for the nearly symmetric ($\eta = 0.2$) and asymmetric ($\eta = 0.6$) potentials. In case (b), the walls are reflected, and eventually stop expanding until the symmetric phase collapses again. In case (c) the field cannot leave the basin of attraction of the broken phase. These plots correspond to different slices of the collisions shown in Fig. 4.

this case, the field approaches after a short while the broken minimum and starts oscillating around it (see Fig. 2(c)). This very much resembles the situation of the tachyonic instability after low-scale inflation.

There are two relevant parameters that decide in which basin of attraction the field ends up. For highly relativistic walls, $\gamma_w \rightarrow \infty$, the field tends to bounce closer to the symmetric phase. The second relevant quantity is the size of the basin of attraction of the symmetric phase. We checked that for a very shallow potential with widely separated minima μ_+ and μ_- [33], reflection is very unlikely due to the huge hierarchy $\mu_+/\mu_- \ll 1$ and as a result the basin of attraction of the symmetric minimum is unattainable.

This situation is demonstrated in Fig. 3, 4 and 5 where we display the results of a simulation of the collision of two planar bubbles in a potential of the form

$$V(\phi) = \lambda(\phi^2 - v^2)^2 + \eta v\phi(\phi^2 - 3v^2). \quad (13)$$

The scalar field obeys the two-dimensional equation of motion

$$\partial_t^2 \phi - \partial_z^2 \phi = -\frac{dV}{d\phi}, \quad (14)$$

and the initial conditions are chosen as bubbles with opposing expansion directions with wall

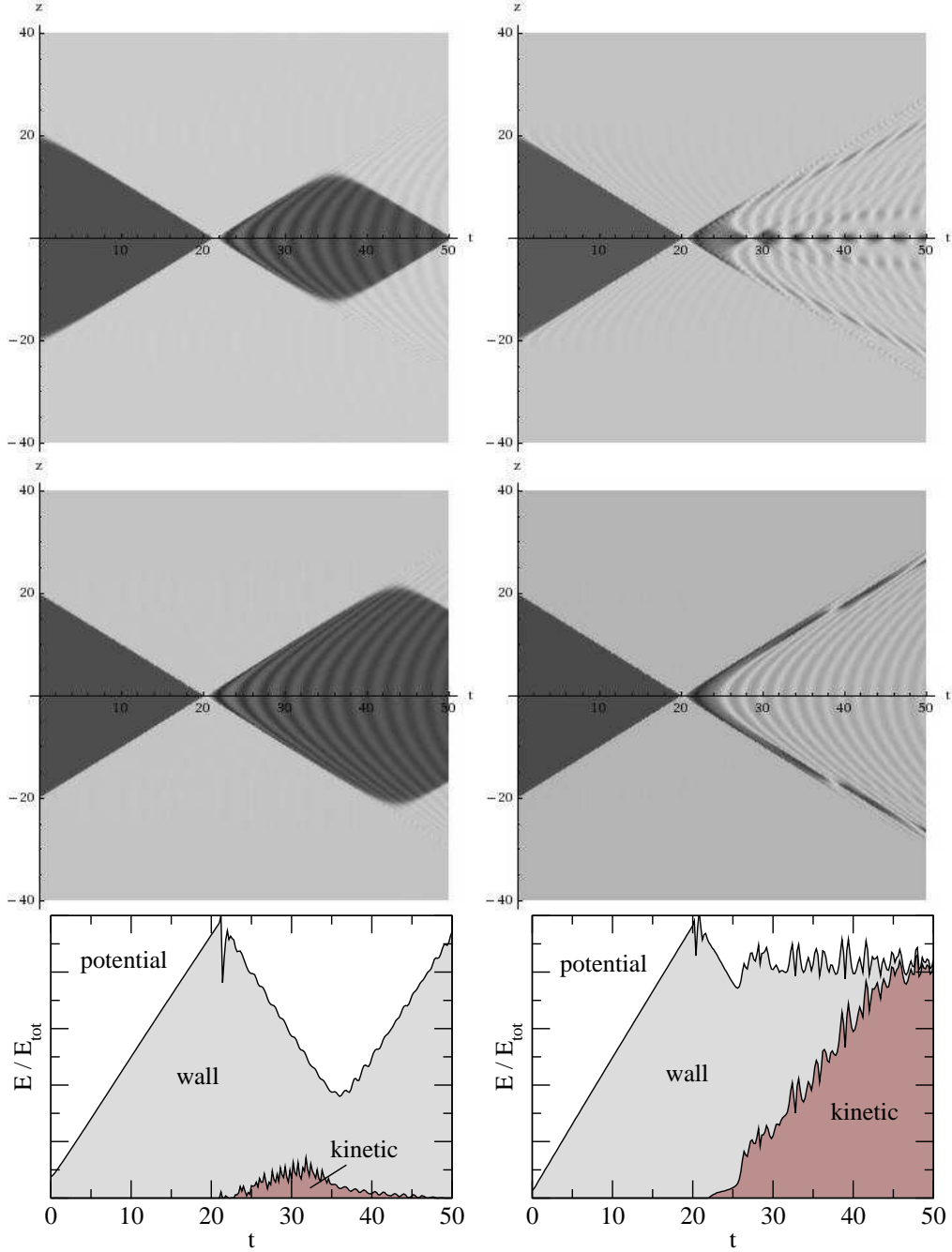


Figure 4: Collision of planar bubble walls for the potential (13) with $\lambda = 1$. The top (bottom) plots use as initial wall velocity $v_w = 0.5$ (0.98), respectively. The left (right) plots are for the symmetric (asymmetric) potential with $\eta = 0.2$ (0.6). Light (dark) gray corresponds to the broken (symmetric) phase. In the left case, the walls are reflected, and eventually stop expanding until the symmetric phase collapses again. In the right case, the field cannot leave the basin of attraction of the broken phase. The last pair of plots shows the time evolution of the fractions of the total energy in potential energy, bubble wall energy and “kinetic” energy of the classical scalar field in the case $v_w = 0.5$ (see text).

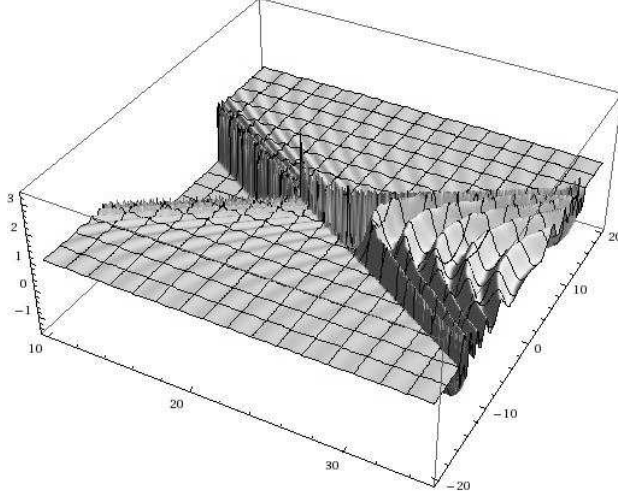


Figure 5: 3D plot corresponding to the bottom right plot of Fig. 4.

thickness l_w and velocity v_w . For a single bubble we use

$$\phi(z, t_0) = \frac{\phi_c}{2} [1 \pm \tanh(\gamma_w [v_w(t - t_0) - (z - z_0)] / l_w)], \quad (15)$$

and we choose the wall thickness to be the value obtained in the thin wall approximation ($l_w^{-1} = \sqrt{2\lambda v}$). The parameter η quantifies the level of degeneracy of the two minima. We show results for the two values $\eta = 0.2$ and $\eta = 0.6$. In the rather symmetric case ($\eta = 0.2$), the walls bounce back to the symmetric phase. In the asymmetric case ($\eta = 0.6$), the field stays in the basin of attraction of the broken phase and starts oscillating around it after a short while of slow roll behavior close to the maximum. Notice that in both cases bubble walls are present after the collision and store the predominant fraction of the vacuum energy. In the asymmetric case, the reflected walls do not lose their energy while expanding into the broken phase and they expand until they meet another reflected wall and thermalize by scattering. We have checked that we obtain similar results for a nearly conformal potential of type (1). The 3D representation of the collision corresponding to the bottom right plot of Fig. 4 is shown in Fig. 5.

In the bottom plots of Fig. 4, we show the fraction of the energy stored in gradient and kinetic energy of the scalar field, since this is the relevant quantity determining the production of winding configurations. What we call “kinetic” is the sum of the gradient plus kinetic energy in the broken phase excluding the wall. Note that the total energy in the asymmetric case is about a factor 3 larger than in the symmetric case (due to the larger difference in the potential minima). Note also that most of the “kinetic” energy in the symmetric case actually results from the wall: When the bubble wall changes direction, the wall becomes thicker and reaches into the region that we attribute to the broken phase (see Fig. 3). From these plots, it is clear that for nearly degenerate minima, there is little energy transferred in kinetic energy of the scalar field whereas for an asymmetric potential (c), a large fraction of the energy ends up in gradient and kinetic energy of the Higgs.

We conclude that bubble collisions in an empty universe as arising in a nearly conformal phase transition lead to a situation that closely resembles the situation after low-scale hybrid

inflation: First, bubbles nucleate and expand. Then, the walls are reflected and sweep space a second time. After the bubble wall has passed a second time, the scalar vev is arranged close to the symmetric phase but beyond the potential barrier of the asymmetric potential (in the basin of attraction of the broken phase). Subsequently the field approaches the broken minimum and releases the potential energy while oscillating around it. After the walls swept all space twice, the scalar field is everywhere in the basin of attraction of the broken phase and reheating begins. The bubble walls collided only once during this early stage and energy drain into the fermionic sector is rather small.

In summary, the important point is that a large kinetic energy is taken from the radion field and drawn into the Higgs sector (we are assuming that there is a sizable coupling between the Higgs and the radion fields). Like in usual preheating the radion has time to oscillate before it decays. This is put by hand in the hybrid inflation model of original cold baryogenesis. In our setup, the radion plays the role of the inflaton. However, we do not have to assume slow-roll since inflation is due to supercooling. Besides, another interesting feature is the little hierarchy between the scale of conformal symmetry breaking and the scale of EW symmetry breaking. Because the energy in the radion sector is large relatively to the Higgs sector, it is easy to produce Higgs winding number by pumping energy from the radion sector.

4 Estimate of the baryon asymmetry

The production of Higgs-winding requires the occurrence of zeroes in the Higgs field. In the simulations of tachyonic preheating, this happens via the self-interactions of the Higgs field and the complexity of the dynamics in the $SU(2)$ gauge space. Our simplistic simulations do not include the gauge structure and we therefore cannot study the production of winding number at the end of the transition. The main point we made in the previous section is that at the end of the transition, almost all the energy of the system resides in the potential and kinetic energy of the scalar field. We believe this makes abundant Higgs winding production very plausible once the gauge structure is included. Compared to the scenario of low-scale hybrid inflation, there is significantly more energy in the scalar sector at this stage since not only the Higgs but also the radion potential energy fuels the scalar dynamics (in slow-roll inflation most of the potential energy of the inflaton is inflated away). In fact, the difficulty might be not to have too much energy in the system and to keep the reheat temperature low enough. The reheating temperature has to be below the temperature T_{EW} at which the electroweak symmetry is restored and at which sphalerons are active in order to prevent the washout of the baryon asymmetry. In models of nearly conformal dynamics at the TeV scale, whether the reheat temperature exceeds T_{EW} actually depends on the Higgs and radion masses, as discussed in detail in [33].

A second difference is in the specific initial conditions. In hybrid inflation, these initial conditions are set by the spinodal instability in the Higgs sector with random orientation in $SU(2)$ gauge space. The Higgs field approaches and oscillates in the Mexican hat potential everywhere more or less at the same time but with a different direction in $SU(2)$ space at different locations. This large degree of disorder leads to the fact that thermalization in the Higgs sector happens relatively fast [34, 59]. In contrast, in our simulations, the time

when the Higgs approaches the potential minimum depends on the position in relation to the colliding bubble walls, and from our plots, the fields appear much more ordered. Clearly, this is due to the fact that we neglect the $SU(2)$ gauge structure, while colliding bubbles with different phases in gauge space lead to magnetic fields and a certain amount of disorder [60]. Still, if two colliding bubbles had the same orientation in gauge space, the problem would effectively become one-dimensional. This should partially suppress the early generation of Higgs winding. Furthermore, due to the lower degree of disorder in gauge space, it is expected that the thermalization of the scalar sector takes a longer time.

Having these differences in mind, we state a rough estimate of the baryon asymmetry in cold electroweak baryogenesis as given in [34, 27]. The estimate is based on the fact that the CP violating operator in eq. (9) can be interpreted (after partial integration) as a chemical potential of the Chern-Simons number

$$\int d^4x \frac{1}{M^2} \phi^\dagger \phi \tilde{F}F \leftrightarrow \int dt \mu_{cs} N_{cs}, \quad (16)$$

of size

$$\mu_{cs} \propto \frac{1}{M^2} \frac{d}{dt} \langle \phi^\dagger \phi \rangle. \quad (17)$$

The resulting estimate for the baryon asymmetry reads [19]

$$\frac{n_B}{s} \propto 3 \times 10^{-5} \frac{v^2}{M^2} \left(\frac{T_{eff}}{T_{rh}} \right)^3, \quad (18)$$

where T_{eff} is the effective temperature of the soft Higgs modes⁴. Ultimately, simulations in the context of inverted hybrid inflation gave the result [27]

$$\frac{n_B}{s} \propto 3 \times 10^{-3} \frac{v^2}{M^2}, \quad (20)$$

corresponding to an effective temperature of order $T_{eff} \simeq 5 T_{rh}$.

This has to be confronted with the experimental constraint on the operator (9) that contributes e.g. to the electric dipole moment of the electron. The arising dipole moment has been estimated to [38]

$$\frac{d_e}{e} \simeq \frac{m_e \sin^2(\theta_W)}{8\pi^2} \frac{1}{M^2} \log \frac{M^2 + m_H^2}{m_H^2}. \quad (21)$$

For a Higgs mass $m_H \sim 200$ GeV, the upper bound on the electric dipole moment [61], $d_e < 1.6 \times 10^{-27} e$ cm, leads to the constraint $M \gtrsim 14$ TeV. Comparison with the estimates (19) and (20) shows that in the present setup baryogenesis is possible as long as the radion fuels the scalar sector with enough energy, which is not a problem as demonstrated in the previous section.

⁴ Using the even more simplistic estimate of [18], one arrives at a smaller asymmetry:

$$\frac{n_B}{s} \propto 4 \times 10^{-6} \frac{v^2}{M^2} \left(\frac{v}{T_{rh}} \right)^3. \quad (19)$$

The form of the new CP violation source will most probably not have a large impact on the result as long as it solely involves the Higgs and gauge fields, as the simulation with a different source in Ref. [44] indicates. Nevertheless, one has to admit that the above estimate can at best predict the early production of Chern-Simons number while for the final baryon asymmetry also the evolution of the Higgs winding plays an important role (this is nicely demonstrated in [27]). An ultimate judgment can at this stage only come from simulations.

5 Conclusion

In the last twelve years, the scenario of cold baryogenesis has been based on a (not particularly motivated) hybrid inflation model. Somehow, it had not been thought of in the context of reheating from bubble collisions. Indeed, first-order phase transitions have been commonly studied based on standard polynomial potentials, in which case the amount of supercooling is not sufficient for cold baryogenesis to work. However, nearly conformal potentials coupled to the Higgs sector, as motivated by a dynamical solution to EW symmetry breaking, can lead to the ideal conditions for a cold electroweak phase transition [33].

We have shown that during bubble collisions, there can be very efficient energy transfer from the bubble wall to the classical Higgs gradient and kinetic energy, hence allowing the production of a large population of winding configurations and non-zero Chern-Simons number. Like in usual EW baryogenesis, the source of baryon number violation is purely Standard Model-like. In this sense, the scenario we propose is based on rather conservative assumptions. The mechanism relies on classical dynamics of the gauge and Higgs field of the Standard Model at the EW phase transition when assuming non-standard CP violating effects (typically through a dimension-six operator involving the time-variation of the Higgs field). Most of the baryon asymmetry is produced when the Higgs is rapidly rolling down its potential, while the gauge fields relax to cancel the gradient energy of the Higgs field.

For the mechanism to work, it is crucial that it takes place in a cold universe, where the coherent bosonic fields can evolve unhindered by the thermal plasma [19]. Besides, the Universe has also to be sufficiently cold after the EW phase transition so that thermal sphalerons production does not wash out the baryon asymmetry produced during preheating. This is the case provided that the radion is relatively light and/or that the Higgs is heavy enough, so that the reheat temperature is naturally below the sphaleron freeze out temperature [33].

Our arguments remain qualitative and we believe they motivate further study. It would be interesting to make numerical simulations similarly to what has been done for hybrid inflation [39, 34, 35, 22–24]. At first sight, this seems impossible in the context of first-order phase transitions, since the problem involves two widely separated scales: The size of the bubbles and the electroweak scale. However, in the case of a nearly conformal potential, the size of the bubbles is no longer important after the first stage of bubble collisions (see Fig. 4) and the simulation of Higgs winding production seems feasible.

Finally, we stress that the underlying theoretical framework we have in mind can be studied in an extra-dimensional context. Holography has proved to be very useful to calculate quantities in strongly coupled theories. We note that there may be interesting related physics concerning the TeV mass skyrmions of [62] which may be abundantly produced at preheating in the way we have shown and could either play a role in baryogenesis or dark matter

generation (as they can be stable).

Acknowledgments

This work is supported by the ERC starting grant Cosmo@LHC (204072).

References

- [1] S. Davidson, E. Nardi, Y. Nir, “Leptogenesis,” *Phys. Rept.* **466** (2008) 105-177. [arXiv:0802.2962 [hep-ph]].
- [2] For recent reviews see e.g. M. G. Schmidt, “Electroweak baryogenesis,” *Prog. Part. Nucl. Phys.* **66** (2011) 249-253 and J. M. Cline, “Baryogenesis,” [hep-ph/0609145].
- [3] V. A. Kuzmin, V. A. Rubakov and M. E. Shaposhnikov, “On The Anomalous Electroweak Baryon Number Nonconservation In The Early Universe,” *Phys. Lett. B* **155**, (1985) 36.
- [4] M. Joyce, T. Prokopec and N. Turok, “Nonlocal electroweak baryogenesis. Part 1: Thin wall regime,” *Phys. Rev. D* **53** (1996) 2930 [arXiv:hep-ph/9410281]. M. Joyce, T. Prokopec and N. Turok, “Nonlocal electroweak baryogenesis. Part 2: The Classical regime,” *Phys. Rev. D* **53** (1996) 2958 [arXiv:hep-ph/9410282].
- [5] F. Csikor, Z. Fodor, J. Heitger, “Endpoint of the hot electroweak phase transition,” *Phys. Rev. Lett.* **82** (1999) 21-24. [hep-ph/9809291].
- [6] M. B. Gavela, P. Hernandez, J. Orloff, O. Pene, “Standard model CP violation and baryon asymmetry,” *Mod. Phys. Lett.* **A9**, 795-810 (1994). [hep-ph/9312215, hep-ph/9312215].
- [7] P. Huet and A. E. Nelson, “Electroweak baryogenesis in supersymmetric models,” *Phys. Rev. D* **53** (1996) 4578 [arXiv:hep-ph/9506477].
- [8] J. M. Cline, M. Joyce and K. Kainulainen, “Supersymmetric electroweak baryogenesis,” *JHEP* **0007** (2000) 018 [arXiv:hep-ph/0006119].
- [9] M. S. Carena, M. Quiros, M. Seco and C. E. M. Wagner, “Improved results in supersymmetric electroweak baryogenesis,” *Nucl. Phys. B* **650**, 24 (2003) [arXiv:hep-ph/0208043].
- [10] T. Konstandin, T. Prokopec, M. G. Schmidt and M. Seco, “MSSM electroweak baryogenesis and flavour mixing in transport equations,” *Nucl. Phys. B* **738**, 1 (2006) [arXiv:hep-ph/0505103].
- [11] V. Cirigliano, S. Profumo and M. J. Ramsey-Musolf, “Baryogenesis, electric dipole moments and dark matter in the MSSM,” *JHEP* **0607** (2006) 002 [arXiv:hep-ph/0603246].

- [12] J. M. Cline, M. Jarvinen, F. Sannino, “The Electroweak Phase Transition in Nearly Conformal Technicolor,” *Phys. Rev.* **D78**, 075027 (2008). [arXiv:0808.1512 [hep-ph]].
M. Jarvinen, T. A. Rytto, F. Sannino, “The Electroweak Phase Transition in Ultra Minimal Technicolor,” *Phys. Rev.* **D79**, 095008 (2009). [arXiv:0903.3115 [hep-ph]].
- [13] P. Creminelli, A. Nicolis and R. Rattazzi, “Holography and the electroweak phase transition,” *JHEP* **0203** (2002) 051 [arXiv:hep-th/0107141].
- [14] L. Randall and G. Servant, “Gravitational Waves from Warped Spacetime,” *JHEP* **0705** (2007) 054 [arXiv:hep-ph/0607158].
- [15] G. Nardini, M. Quiros and A. Wulzer, “A Confining Strong First-Order Electroweak Phase Transition,” *JHEP* **0709** (2007) 077 [arXiv:0706.3388 [hep-ph]].
- [16] T. Konstandin, G. Nardini and M. Quiros, “Gravitational Backreaction Effects on the Holographic Phase Transition,” arXiv:1007.1468 [hep-ph].
- [17] J. R. Espinosa, T. Konstandin, J. M. No and G. Servant, “Energy Budget of Cosmological First-order Phase Transitions,” *JCAP* **1006** (2010) 028 [arXiv:1004.4187 [hep-ph]].
- [18] L. M. Krauss, M. Trodden, “Baryogenesis below the electroweak scale,” *Phys. Rev. Lett.* **83** (1999) 1502-1505. [hep-ph/9902420].
- [19] J. Garcia-Bellido, D. Y. Grigoriev, A. Kusenko and M. E. Shaposhnikov, “Non-equilibrium electroweak baryogenesis from preheating after inflation,” *Phys. Rev. D* **60**, 123504 (1999) [arXiv:hep-ph/9902449].
- [20] E. J. Copeland, D. Lyth, A. Rajantie and M. Trodden, “Hybrid inflation and baryogenesis at the TeV scale,” *Phys. Rev. D* **64**, 043506 (2001) [arXiv:hep-ph/0103231].
- [21] J. M. Cornwall, D. Grigoriev, A. Kusenko, “Resonant amplification of electroweak baryogenesis at preheating,” *Phys. Rev.* **D64** (2001) 123518. [hep-ph/0106127].
- [22] J. Smit and A. Tranberg, “Chern-Simons number asymmetry from CP-violation during tachyonic preheating,” arXiv:hep-ph/0210348.
- [23] J. Garcia-Bellido, M. Garcia-Perez and A. Gonzalez-Arroyo, “Chern-Simons production during preheating in hybrid inflation models,” *Phys. Rev. D* **69**, 023504 (2004) [arXiv:hep-ph/0304285].
- [24] A. Tranberg and J. Smit, “Baryon asymmetry from electroweak tachyonic preheating,” *JHEP* **0311**, 016 (2003) [arXiv:hep-ph/0310342].
- [25] B. J. W. van Tent, J. Smit and A. Tranberg, “Electroweak-scale inflation, inflaton-Higgs mixing and the scalar spectral index,” *JCAP* **0407** (2004) 003 [arXiv:hep-ph/0404128].
- [26] M. van der Meulen, D. Sexty, J. Smit and A. Tranberg, “Chern-Simons and winding number in a tachyonic electroweak transition,” *JHEP* **0602** (2006) 029 [arXiv:hep-ph/0511080].

- [27] A. Tranberg, J. Smit and M. Hindmarsh, “Simulations of Cold Electroweak Baryogenesis: Finite time quenches,” *JHEP* **0701** (2007) 034 [arXiv:hep-ph/0610096].
- [28] K. Enqvist, P. Stephens, O. Taanila and A. Tranberg, “Fast Electroweak Symmetry Breaking and Cold Electroweak Baryogenesis,” arXiv:1005.0752 [astro-ph.CO].
- [29] L. Randall and R. Sundrum, “A large mass hierarchy from a small extra dimension,” *Phys. Rev. Lett.* **83** (1999) 3370 [arXiv:hep-ph/9905221].
- [30] W. D. Goldberger and M. B. Wise, “Modulus stabilization with bulk fields,” *Phys. Rev. Lett.* **83**, 4922 (1999) [arXiv:hep-ph/9907447].
- [31] N. Arkani-Hamed, M. Porrati and L. Randall, “Holography and phenomenology,” *JHEP* **0108**, 017 (2001) [arXiv:hep-th/0012148].
- [32] R. Rattazzi and A. Zaffaroni, “Comments on the holographic picture of the Randall-Sundrum model,” *JHEP* **0104** (2001) 021 [arXiv:hep-th/0012248].
- [33] T. Konstandin and G. Servant “Cosmological consequences of nearly conformal dynamics at the TeV scale” [arXiv:1104.4791 [hep-ph]].
- [34] G. N. Felder, J. Garcia-Bellido, P. B. Greene, L. Kofman, A. D. Linde and I. Tkachev, “Dynamics of symmetry breaking and tachyonic preheating,” *Phys. Rev. Lett.* **87** (2001) 011601 [arXiv:hep-ph/0012142].
- [35] J. Garcia-Bellido, M. Garcia Perez and A. Gonzalez-Arroyo, “Symmetry breaking and false vacuum decay after hybrid inflation,” *Phys. Rev. D* **67**, 103501 (2003) [arXiv:hep-ph/0208228].
- [36] N. Turok, “Global Texture as the Origin of Cosmic Structure,” *Phys. Rev. Lett.* **63** (1989) 2625.
- [37] N. Turok and J. Zadrozny, “Dynamical generation of baryons at the electroweak transition,” *Phys. Rev. Lett.* **65**, 2331 (1990).
- [38] A. Lue, K. Rajagopal and M. Trodden, “Semi-analytical approaches to local electroweak baryogenesis,” *Phys. Rev. D* **56** (1997) 1250 [arXiv:hep-ph/9612282].
- [39] A. Rajantie, P. M. Saffin, E. J. Copeland, “Electroweak preheating on a lattice,” *Phys. Rev. D* **63** (2001) 123512. [hep-ph/0012097].
- [40] M. E. Shaposhnikov, “Possible Appearance of the Baryon Asymmetry of the Universe in an Electroweak Theory,” *JETP Lett.* **44** (1986) 465-468.
- [41] M. E. Shaposhnikov, “Baryon Asymmetry of the Universe in Standard Electroweak Theory,” *Nucl. Phys.* **B287** (1987) 757-775.
- [42] J. Smit, “Effective CP violation in the standard model,” *JHEP* **0409** (2004) 067. [hep-ph/0407161].

- [43] A. Hernandez, T. Konstandin and M. G. Schmidt, “Sizable CP Violation in the Bosonized Standard Model,” Nucl. Phys. B **812**, 290 (2009) [arXiv:0810.4092 [hep-ph]].
- [44] A. Tranberg, A. Hernandez, T. Konstandin and M. G. Schmidt, “Cold electroweak baryogenesis with Standard Model CP violation,” Phys. Lett. B **690**, 207 (2010) [arXiv:0909.4199 [hep-ph]].
- [45] A. Tranberg, “Standard Model CP-violation and Cold Electroweak Baryogenesis,” arXiv:1009.2358 [hep-ph].
- [46] C. Garcia-Recio, L. L. Salcedo, “CP violation in the effective action of the Standard Model,” JHEP **0907** (2009) 015. [arXiv:0903.5494 [hep-ph]].
- [47] L. L. Salcedo, “Leading order one-loop CP and P violating effective action in the Standard Model,” Phys. Lett. **B700** (2011) 331-335. [arXiv:1102.2400 [hep-ph]].
- [48] M. Dine, P. Huet, R. L. . Singleton and L. Susskind, “Creating the baryon asymmetry at the electroweak phase transition,” Phys. Lett. B **257**, 351 (1991).
- [49] M. Dine, P. Huet and R. L. . Singleton, “Baryogenesis at the electroweak scale,” Nucl. Phys. B **375**, 625 (1992).
- [50] A. G. Cohen, D. B. Kaplan and A. E. Nelson, “Diffusion Enhances Spontaneous Electroweak Baryogenesis,” Phys. Lett. B **336** (1994) 41 [arXiv:hep-ph/9406345].
A. G. Cohen, D. B. Kaplan and A. E. Nelson, “Progress in electroweak baryogenesis,” Ann. Rev. Nucl. Part. Sci. **43** (1993) 27 [arXiv:hep-ph/9302210].
- [51] D. Bodeker and G. D. Moore, “Can electroweak bubble walls run away?,” JCAP **0905**, 009 (2009) [arXiv:0903.4099 [hep-ph]].
- [52] A. Kosowsky and M. S. Turner, “Gravitational Radiation From Colliding Vacuum Bubbles: Envelope Approximation To Many Bubble Collisions,” Phys. Rev. D **47** (1993) 4372 [arXiv:astro-ph/9211004].
- [53] R. Watkins and L. M. Widrow, “Aspects of reheating in first order inflation,” Nucl. Phys. B **374** (1992) 446.
- [54] S. W. Hawking, I. G. Moss and J. M. Stewart, “Bubble Collisions In The Very Early Universe,” Phys. Rev. D **26**, 2681 (1982).
- [55] E. W. Kolb and A. Riotto, “Preheating and symmetry restoration in collisions of vacuum bubbles,” Phys. Rev. D **55**, 3313 (1997) [arXiv:astro-ph/9602095].
- [56] E. W. Kolb, A. Riotto, I. I. Tkachev, “Evolution of the order parameter after bubble collisions,” Phys. Rev. **D56** (1997) 6133-6138. [astro-ph/9703119].
- [57] J. T. Giblin, L. Hui, E. A. Lim and I. S. Yang, “How to Run Through Walls: Dynamics of Bubble and Soliton Collisions,” arXiv:1005.3493 [hep-th].

- [58] R. Easther, J. T. Giblin, L. Hui and E. A. Lim, “A New Mechanism for Bubble Nucleation: Classical Transitions,” *Phys. Rev. D* **80**, 123519 (2009) [arXiv:0907.3234 [hep-th]].
- [59] J. -I. Skullerud, J. Smit, A. Tranberg, “W and Higgs particle distributions during electroweak tachyonic preheating,” *JHEP* **0308** (2003) 045. [hep-ph/0307094].
- [60] T. W. B. Kibble, A. Vilenkin, “Phase equilibration in bubble collisions,” *Phys. Rev. D* **52** (1995) 679-688. [hep-ph/9501266].
- [61] B. C. Regan, E. D. Commins, C. J. Schmidt and D. DeMille, “New limit on the electron electric dipole moment,” *Phys. Rev. Lett.* **88** (2002) 071805.
- [62] A. Pomarol, A. Wulzer, “Stable skyrmions from extra dimensions,” *JHEP* **0803**, 051-051 (2008). [arXiv:0712.3276 [hep-th]].